

Numerical modeling of enhanced biodenitrification in a laboratory flow-through experiment

Alex Abu (1,2*), Cristina Domènech (1,2) Raúl Carrey (2,3), Rosanna Margalef-Martí (4), Neus Otero (1,2)

(1) Grup MAiMA, SGR Mineralogia Aplicada, Geoquímica i Geomicrobiologia, Departament de Mineralogia, Petrologia i Geologia Aplicada, Facultat de Ciències de La Terra, Universitat de Barcelona (UB), 08028, Barcelona, Catalonia, Spain

(2) Institut de Recerca de l'Aigua (IdRA), Universitat de Barcelona (UB), 08001, Barcelona, Catalonia, Spain

(3) Centres Científics i Tecnològics, Universitat de Barcelona (UB), C/Lluís Solé i Sabarís 1-3, 08028 Barcelona (Spain)

(4) Université de Pau et des Pays de l'Adour, E2S UPPA, Institut des Sciences Analytiques et de Physico-chimie pour l'Environnement et les matériaux (IPREM), Pau, France

*corresponding author: alexabu@ub.edu

Keywords: Denitrification, Biostimulation, Isotopic fractionation, Biogeochemical model

INTRODUCTION

High concentration of nitrate (NO_3^-) in water resources has become a widespread and important environmental contaminant, being anthropogenic nitrogen input the principal source of NO_3^- pollution (Arauzo, 2017). Under anaerobic conditions, microbial reduction of NO_3^- to $\text{N}_{2(g)}$ to oxidize dissolved organic carbon (DOC) is the principal NO_3^- attenuation process in groundwater aquifers (Matchett et al., 2019). Enhanced biodenitrification approach, has been adopted to create optimized conditions by providing an external electron donor source in aquifers to overcome the natural limitation of DOC. Denitrification phenomena usually result in kinetic isotope fractionation (ϵ) on the N and O isotopes (Chen and MacQuarrie, 2005) providing an effective tool to quantify the evolution of denitrification processes. In this context, Margalef-Martí et al., (2019) studied the ability of whey to enhance biodenitrification in NO_3^- polluted aquifers through a laboratory flow-through experiment (Figure 1A). In this abstract, we present the numerical modeling of part of the experimental data of Margalef-Martí et al. (2019). The understanding of the different processes occurring in the system and the ability of reproducing them numerically is the first step to upscale the treatments to field scale (Rodríguez-Escales et al., 2014).

METHODOLOGY

The GibbsStudio software (Nardi and de Vries, 2017) based on PHREEQC code (Parkhurst and Appelo, 2013) and the iso.dat thermodynamic database from PHREEQC were used for reactive transport calculations. The main processes considered in the model are nitrate respiration ($\text{NO}_3^- + 2\text{H}^+ + 2\text{e}^- \rightarrow \text{NO}_2^- + \text{H}_2\text{O}$, Reaction 1), nitrite respiration ($\text{NO}_2^- + 4\text{H}^+ + 3\text{e}^- \rightarrow \frac{1}{2}\text{N}_2 + 2\text{H}_2\text{O}$, Reaction 2), DOC (as CH_2O) oxidation ($\text{CH}_2\text{O} + 2\text{H}_2\text{O} \rightarrow \text{HCO}_3^- + 5\text{H}^+ + 4\text{e}^-$, Reaction 3), ^{15}N - NO_3^- disappearance ($[^{15}\text{N}\text{-NO}_3^-] \rightarrow [^{15}\text{N}\text{-NO}_2^-]$, Reaction 4) and ^{15}N - NO_2^- disappearance ($[^{15}\text{N}\text{-NO}_2^-] \rightarrow [^{15}\text{N}\text{-N}_2]$, Reaction 5) which are considered to be kinetically controlled.

RESULTS AND DISCUSSION

Conservative Br⁻ tracer test performed before the biostimulation experiment was used to calibrate the system hydraulic properties and performance in the modeling (Figure 1B). In the system anaerobic conditions, the oxidation of the DOC by an electron acceptor source provides the microbial community with energy for growth and cell synthesis. Reactions 1 and 2 were modelled according to a dual Monod kinetic expression (eq.1) depending on the concentrations (in mol/dm³) of the electron acceptor (NO_3^- or NO_2^-), of the electron donor CH_2O and of the biomass community responsible for each reaction ($[X]$), whose growth and decay was also considered (eq.2). The $\delta^{15}\text{N}$ of NO_3^- and NO_2^- was modelled according to eq. 3, linked to NO_3^- or NO_2^- evolution.

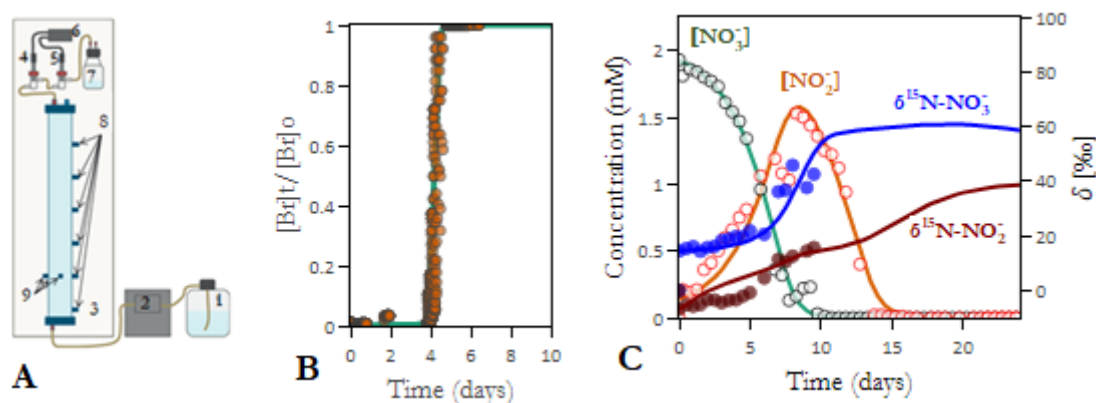


Figure 1. (A) Scheme of the experimental setup. 1) inflow reservoir, 2) peristaltic pump, 3) isothermal chamber 4) Eh probe, 5) pH probe, 6) multiparametric analyzer, 7) outflow water, 8) sampling points along column 9) injection points. (B) Conservative Br tracer test results. (C) NO₃⁻ and NO₂⁻ concentration and N isotope fractionation. Dots = experimental data measurements, line = fitted model.

$$R_{EA} = -q_{\max} [X] \left(\frac{[EA]}{[EA] + k_{EA}} \right) \left(\frac{[CH_2O]}{[CH_2O] + k_{CH_2O}} \right) \quad (1)$$

$$R_X = -Y_h R_{EA} - b[X] \quad (2)$$

$$R_{^{15}N} = R_{EA} \frac{[^{15}N]}{[^{14}N]} (\epsilon + 1) \quad (3)$$

As shown in Figure 1C, experimental values have been reproduced by considering a q_{\max} value of $1 \cdot 10^{-7}$ mol/g cell/s, k_{EA} of $5 \cdot 10^{-4}$ mol/L and k_{CH_2O} of $2.2 \cdot 10^{-5}$ mol/L for NO₃⁻ reduction and q_{\max} value of $1 \cdot 10^{-7}$ mol/g cell/s, k_{EA} of $6 \cdot 10^{-4}$ mol/L, k_{CH_2O} of $3 \cdot 10^{-5}$ mol/L for NO₂⁻ reduction. b value of $1 \cdot 10^{-7}$ /s and Y_h , of 60 g cell/mol were considered for both NO₃⁻ and NO₂⁻ reduction. ϵ values of -9 ‰ and -4 ‰ were considered for nitrate and nitrite reduction respectively. NO₃⁻ continuously decreased achieving complete reduction, NO₂⁻ increased to a peak and decreased afterwards. ¹⁵N isotopes progressively increased as nitrate and nitrite concentration decreased.

CONCLUSIONS

In the experimental conditions used, the concentration and isotope evolution of the column flow-through experiment of Margalef-Martí et al. (2019) have been reproduced by the conceptual and numerical model presented in this study. Although a preliminary set of constants have been fitted, they must be tested with additional experimental data sets. However, this model opens the opportunity to upscale the treatment at bigger scales.

REFERENCES

- Arauzo, M. (2017): Vulnerability of groundwater resources to nitrate pollution: A simple and effective procedure for delimiting Nitrate Vulnerable Zones. *Sci. Total Environ.* 575, 799–812.
- Chen, D.J. & MacQuarrie, K.T. (2005): Correlation of $\delta^{15}N$ and $\delta^{18}O$ in NO₃⁻ during denitrification in groundwater. *J. Environ. Eng. Sci.* 4, 221–226.
- Margalef-Martí, R., Carrey, R., Soler, A. & Otero, N. (2019): Evaluating the potential use of a dairy industry residue to induce denitrification in polluted water bodies: A flow-through experiment. *J. Environ. Manage.* 245, 86–94.
- Matchett, L.S., Goulding, K.W.T., Webster, C.P. & Haycock, N.E. (2019): Denitrification in riparian buffer zones: the role of floodplain hydrology 13, 10–11.
- Nardi, A. & de Vries, L.M. (2017): GibbsStudio, Barcelona Science Technologies SL, Barcelona, Spain. Retrieved from <https://gibbsstudio.io/>
- Parkhurst, D.L. & Appelo, C.A.J. (2013): Description of input and examples for PHREEQC version 3—a computer program for speciation, batch-reaction, one-dimensional transport, and inverse geochemical calculations. USGS Techniques and Methods, book 6, chap. A43, 497 p., available at <http://pubs.usgs.gov/tm/06/A43/>.
- Rodríguez-Escales, P., Breukelen, B.M. Van, Vidal-Gavilan, G., Soler, A. & Folch, A. (2014): Integrated modeling of biogeochemical reactions and associated isotope fractionations at batch scale: A tool to monitor enhanced biodenitrification applications. *Chem. Geol.* 365, 20–29.